Lasers in Manufacturing Conference 2015

Laser welding inspection on aeronautic material with non-contact real-time optical beam deflection sensor

João M. S. Sakamoto[a,*], Renan B. Marques[b], Rudimar Riva[a], Cláudio Kitano[c], Gefeson M. Pacheco[d]

[a]*Instituto de Estudos Avançados (IEAv), Trevo Cel. Av. José A. A. do Amarante 1, São José dos Campos SP 12228-001, Brazil*
[b]*Universidade Federal de São Paulo (Unifesp), Av. Cesare Mansueto Giulio Lattes 1201, São José dos Campos SP 12247-014, Brazil*
[c]*Universidade Estadual Paulista (UNESP), Av. Professor José Carlos Rossi 1370 Campus III, Ilha Solteira SP 15385-000, Brazil*
[d]*Instituto Tecnológico de Aeronáutica (ITA), Praça Mal. Eduardo Gomes 50, São José dos Campos SP 12228-900, Brazil*

Abstract

In this work we show the application of an optical beam deflection sensor for detection of airborne thermal and acoustic waves generated by laser welding of aeronautical aluminum (AA 6013), and the sensor's potential for process inspection and control. The principle of working of the sensor is based in the measurement of the refractive index variation (of the surrounding medium) induced by temperature or pressure variation. The laser welding conditions generates the index variation which, in turn, deflects the optical beam, modulating the optical intensity. Therefore, the sensor is able to perform non-contact, non-destructive and surface roughness independent measurements.

Keywords: optical beam deflection; real-time; mirage effect; photothermal deflection; non-contact inspection.

1. Introduction

The laser welding application in industry has being increased since it can provide weight reduction (e.g. replacing rivets), fast production, robot compatibility, welding of dissimilar materials, and so on. As a consequence, the inspection of the laser welded part is essential to guarantee safety and reliability mainly in aerospace/aeronautics and automotive applications.

* Corresponding author. Tel.: +55-12-3947-5435; fax: +55-12-3944-1177.
E-mail address: sakamoto@ieav.cta.br.

Different techniques for welding inspection have being developed based, for example, in spectroscopy or plasma plume optical intensity analysis (Ancona 2001, Fox 2001, Bardin 2005, Sibillano 2009, Sibillano 2010). In this work we present an alternative optical sensor, based in the optical beam deflection caused by the airborne thermal and acoustic waves generated by laser welding. The sensor's principle of working and a brief theory are presented with both simulated and experimental characteristic curves. In addition, we show the application of the sensor for detection of signals from an aeronautical aluminum (AA 6013) sample, welded by laser, and the sensor's potential for process inspection and control.

2. Working principle

The working principle of the optical beam deflection sensor is based in the angular variation of an optical beam crossing a region under refractive index variation caused by temperature (mirage effect) or pressure. According to (Rodrigues 1990), the gradient of the refractive index is given by:

$$\frac{\partial n}{\partial y} = \frac{\partial n}{\partial p}\frac{\partial p}{\partial y} + \frac{\partial n}{\partial T}\frac{\partial T}{\partial y}, \qquad (1)$$

where p is the pressure and T is the temperature. Still according to (Rodrigues 1990), the deflection angle is given by:

$$\theta = \frac{L}{n_o}\left[\frac{\partial n}{\partial y}\right]_{y=y_o}, \qquad (2)$$

where n_o is the refractive index of the surrounding medium at room temperature and pressure, and y_o is the beam offset (distance from the sample surface and the sensor beam). The parameter L is the length of the region of interaction between the sensor beam and the refractive index gradient, as shown in Fig. 1.

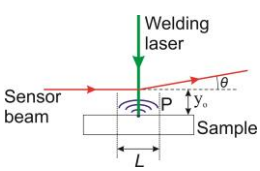

Fig. 1. Sensor beam deflection by refractive index gradient.

The sensor proposed in this work comprises a laser, two flat mirrors (M_1 and M_2), a polarizing beam-splitter (PBS), a quarter wave plate (λ/4), a positive lens (L), a knife-edge (KE), a band-pass optical filter (centered on the sensor laser wavelength), and a photodetector (PD) with a transimpedance circuit. This components are arranged as shown in Fig. 2.

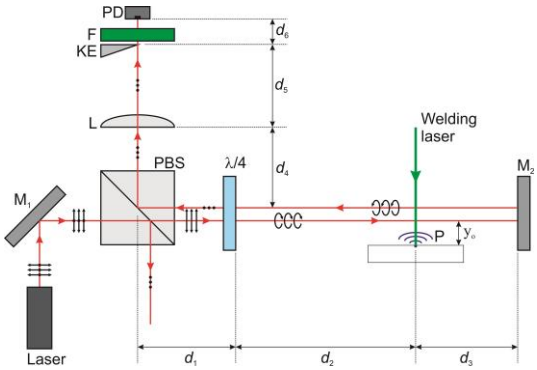

Fig. 2. Sensor setup.

The parameter d_1 is the distance between the PBS center and the quarter-wave plate; d_2 is the distance between the quarter-wave plate and the point P where the variation in the refractive index occurs; d_3 is the distance between P and M_2; d_4 is the distance between the center of the PBS and L; d_5 is the distance between L and KE; and d_6 is the distance between KE and PD. The beam that goes from the PBS to M_2 is collinear with the beam that goes back, from M_2 to PBS. In Fig. 2, however, they are shown separately for a better understanding of the setup.

The components of the sensor are placed in order to avoid light feedback to the laser. Therefore, the PBS and the quarter-wave plate are used together to direct the laser beam from the laser to the region P and, in the opposite way, to direct the returning beam to the PD, as follows: the laser beam is not polarized and it is directed by M_1 to the PBS which, in turn, separates the horizontal (represented by three arrows) and vertical (represented by three dots) polarizations. The vertical polarization is not used, while the horizontal polarization travels to the quarter-wave plate. The optical axis of this plate is rotated at 45° degrees in relation to the laser polarization, in order to turn the polarization to circular. In the region between the quarter-wave plate and the mirror M_2, the beam crosses the perturbation P in the refractive index (caused by the laser welding), which deviates the beam by an angle θ. After being reflected by M_2, the beam keeps the circular polarization, but in the opposite direction. The beam thus crosses the region P again and is deflected once more by θ. After crossing the quarter-wave plate, the beam emerges with vertical polarization (orthogonal to the input polarization) and is deflected by PBS in direction of the positive lens. The lens focuses the beam, which can be partially obstructed by the knife-edge, and crosses the filter F, to avoid wavelengths other than the sensor laser one impinge on the photodetector.

In summary, the perturbation P causes an angular deviation θ on the beam, which makes the optical spot translate over the PD area. This, in turn, causes an intensity modulation on the light detected by the PD.

3. Theory

In this section, we show the procedures to obtain the characteristic curve of the sensor. Thus, the first step to accomplish that is to determine the position Y of the optical spot on the photodetector plane. After that, the integration of the optical intensity over the PD can be evaluated as function of the angle θ. Thus, in order to determine the spot position Y, the ABCD matrix was evaluated, based in the setup shown in Fig. 2, regarding that the perturbation P imposes an angular variation twice in the laser beam (one for each beam pass). Therefore, we have the following ABCD matrix:

$$\begin{bmatrix} Y \\ \alpha \end{bmatrix} = \begin{bmatrix} 1 & d_6 \\ 0 & 1 \end{bmatrix} \begin{bmatrix} 1 & d_5 \\ 0 & 1 \end{bmatrix} \begin{bmatrix} 1 & 0 \\ -1/f & 1 \end{bmatrix} \begin{bmatrix} 1 & d_4 \\ 0 & 1 \end{bmatrix} \begin{bmatrix} 1 & d_1 \\ 0 & 1 \end{bmatrix} \begin{bmatrix} 2\theta(d_2 + d_3) \\ 2\theta \end{bmatrix}. \quad (3)$$

Equation 3 can then be used to determine the Y position of the optical spot. In the case where the PD is located at the lens focus, i.e., $d_5 + d_6 = f$, the value of Y in Eq. (3) can be simplified to:

$$Y = 2f\theta, \quad (4)$$

which show us, in this case, that the spot position becomes independent of the sensor geometrical parameters as d_1, d_2, d_3, d_4, d_5, and d_6. Therefore, this configuration can be suitable for this type of sensor when a lower sensitivity is acceptable (the sensor's sensitivity decreases for $Y = 2f\theta$ - this will not be addressed in this work).

The second step is to determine the characteristic equation of the sensor. Regarding that the optical spot has a Gaussian intensity profile and that it is translated by a distance Y, we have that

$$I(x,y) = \frac{2P_i}{\pi w^2} \exp\left\{\frac{-2}{w^2}\left[x^2 + (y+Y)^2\right]\right\}, \quad (5)$$

where x is the horizontal coordinate, y the vertical coordinate, P_i is the optical spot total power, and w is the spot radius.

The power gathered by the PD is given by the integral of the intensity over the PD area as $P_o = \int I(x,y)dS$, where $dS = dxdy$. Therefore, the power transfer coefficient, defined as $\eta = P_o/P_i$, can be evaluated as

$$\eta = \frac{P_o}{P_i} = \frac{2}{\pi w}\sqrt{\frac{\pi}{2}}\int_{-a_r}^{a_r} \exp\left[\frac{-2}{w^2}(y+Y)^2\right] \cdot erf\left(\frac{\sqrt{2}}{w}\sqrt{a_r^2 - y^2}\right) dy, \quad (6)$$

where a_r is the PD radius. To account for the KE, the integration limit in Eq. 6 should be changed to the one corresponding to the KE position, e.g., if KE is in the center of the PD (blocking half of the PD area) the integration limits range from 0 to a_r.

4. Results

An experimental setup was mounted to determine the characteristic curve of the sensor. This was accomplished by rotating the mirror M_2 in order to simulate a variation in the angle θ. Although the θ variation occurs in the region P, it can be shown that it is equivalent to the variation in the angle θ of the mirror M_2. The result is shown in Fig. 3.

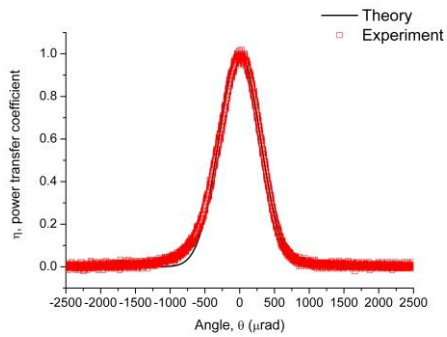

Fig. 3. Experimental and theoretical characteristic curves of the optical beam deflection sensor.

The characteristic curve presents two linear regions that can be used to detect dynamic variations in θ around the sensor's operation point. The normalized sensitivity of this sensor is ($2V_{\max}$) mV/μrad, the linear range is 234 μrad, and the operation point is set at $0.5V_{\max}$. The parameter $V_{\max}$ corresponds to the output voltage at the sensor's peak and it is measured in units of volts. In our setup it was measured as $V_{\max}$ = 4 V and, thus, the sensitivity (unnormalized) was equal to 8 mV/μrad. In order to detect dynamic angular (θ) variations, the sensor was set on the operation point by imposing an angle θ which gives an output voltage of half $V_{\max}$, in our case, 2 V.

Another experimental setup was mounted to verify the detection of thermal and acoustic waves generated by a laser, where the sample and the sensor were positioned as shown in Fig. 2. First of all, we detected the signals generated by a ytterbium fiber laser operating at 1060 nm, in pulsed regime with pulsewidth of 200 ns, repetition rate of 20 kHz, and average power of 20 W. The laser pulses and the signals detected by the sensor are shown in Fig. 4.

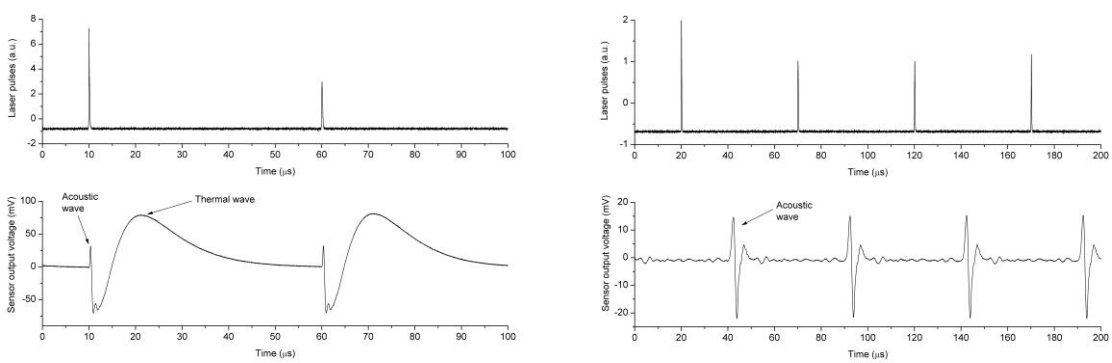

(a) (b)

Fig. 4. Signals detected by the sensor, generated by a pulsed laser. (a) Sensor beam in the vicinity of the sample surface ($y_o \approx 0$ mm). (b) Sensor beam above the sample surface ($y_o \approx 5.5$ mm).

This result indicated that the sensor is able to detect pressure (acoustic) and thermal waves generated by the laser. Besides, as seen on Fig. 4 (b), increasing the beam offset, y_o, one can decrease the influence of the thermal wave. Therefore, in the next experiment, we used an aeronautical aluminum (AA 6013) plate with

1.0 mm of thickness. The beam offset was set as y_o = 3.5 mm. The welding laser was another ytterbium fiber laser at 1060 nm and 800 W on CW operation. The sample translation velocity was 50 mm/s, the length of the welding was 70 mm, and the laser position was varied from -7 mm to 7 mm in relation to its focus. The signal was acquired without averaging, and it is shown in function of position in Fig. 5 (a), with its Short-Time Fourier Transform (STFT).

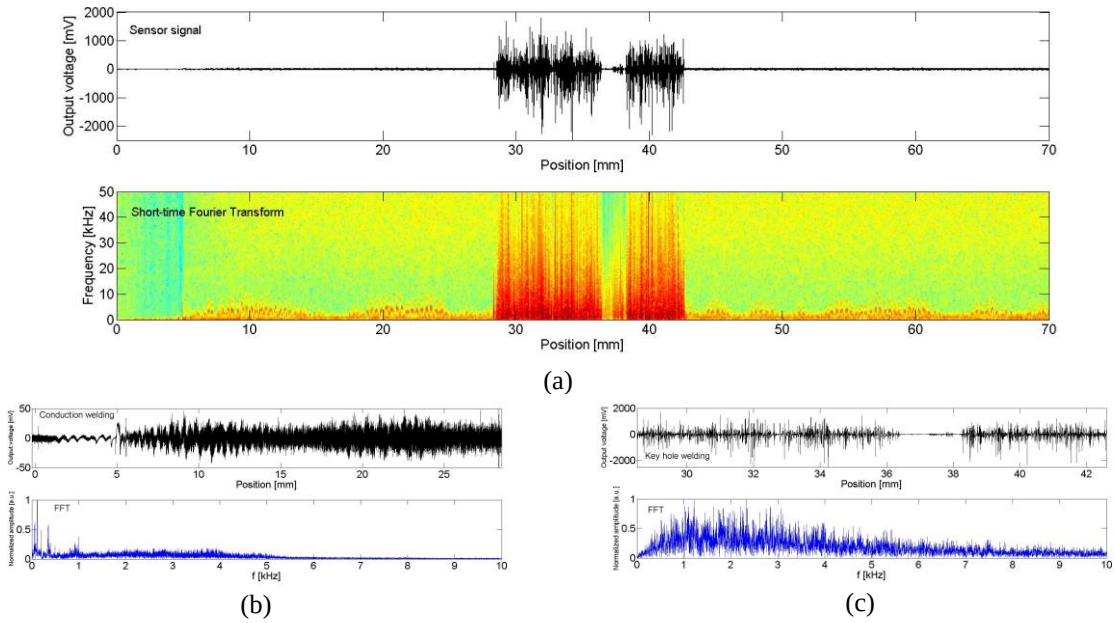

Fig. 5. Signal detected by the sensor on laser welding. (a) Signal and STFT. (b) Conduction welding part. (c) Keyhole welding part.

The signal acquired presented two distinct welding regimes: one corresponding to the conduction welding (from 0 mm to 28.5 mm and from 42.6 mm to 70 mm) and the other, to the keyhole welding (from 28.5 mm to 42.6 mm). The region from 0 mm to 28.5 mm is shown in Fig. 5 (b) with its Fast Fourier Transform (FFT), where there are well defined frequency components bellow 1 kHz. The region from 28.5 mm to 42.6 mm is shown if Fig. 5 (c) with its FFT, which presents an overall increase in the spectrum magnitude in the region bellow approximately 5 kHz. It is noteworthy that the DC component of both signals was filtered. The spectrums of the two regions indicate a different signature for conduction or keyhole welding regimes, which is the first step to investigate the signals characteristics in order to seek for welding defects.

5. Conclusions

The results obtained in this work show the capability of the optical beam deflection sensor for detecting refractive index variations due to thermal or acoustic waves generated by a welding laser. Also, the sensor detected distinct welding regimes, as the conduction or keyhole, presenting a potential for real-time, non-destructive and non-contact inspection and control for laser welding.

Acknowledgements

The authors would like to thank the Brazilian agency CNPq for funding of this research (process number 485147/2013-0), and the Brazilian funding agencies CNPq and FAPESP (INCT de Estudos do Espaço, 2008/57866-1) for partial funding of this research.

References

Rodrigues, N. A. S., Miranda, L. C. M., 1990. Thermoelectric amplification of acoustic waves observed in Ni using optical-beam-deflection detection, Physical Review B 42, p. 1177.

Sibillano, T., Ancona, A., Berardi, V., Lugarà, P. M., 2009. A real-time spectroscopic sensor for monitoring laser welding processes, Sensors 9, p. 3376.

Sibillano, T., Ancona, A., Rizzi, D., Lupo, V., Tricarico, L., Lugarà, P. M., 2010. Plasma plume oscillations monitoring during laser welding of stainless steel by Discrete Wavelet Transform application, Sensors 10, p. 3549.

Ancona, A., Spagnolo, V., Lugarà, P. M., Ferrara, M., 2001. Optical sensor for real-time monitoring of CO_2 laser welding process, Applied Optics 40, p. 6019.

Fox, M. D. T., Peters, C., Blewett, I. J., Hand, D. P., Jones, J. D. C., 2001. Real-time, nonintrusive oxidation detection system for the welding of reactive aerospace materials, Applied Optics 40, p. 6606.

Bardin, F., Cobo, A., Lopez-Higuera, J. M., Collin, O., Aubry, P., Dubois, T., Högström, M., Nylen, P., Jonsson, P., Jones, J. D. C., Hand, D. P., 2005. Optical techniques for real-time penetration monitoring for laser welding, Applied Optics 44, p. 3869.